

J. Electroanal. Chem., 223 (1987) 25–50
Elsevier Sequoia S.A., Lausanne – Printed in The Netherlands

Review

IMPEDANCE SPECTROSCOPY AND ITS USE IN ANALYZING THE STEADY-STATE AC RESPONSE OF SOLID AND LIQUID ELECTROLYTES *

J. ROSS MACDONALD

Department of Physics and Astronomy, University of North Carolina, Chapel Hill, NC 27514 (U.S.A.)

(Received 24th November 1986)

ABSTRACT

Impedance spectroscopy is defined and some of its applications illustrated for both liquid and solid electrolyte situations. Particular emphasis is placed on complex least squares fitting of small-signal frequency response data at various immittance levels. Most such response data must be fit to an equivalent electrical circuit since a detailed microscopic model of the response is usually lacking. It is found for most ionic response data, as well as that from purely dielectric systems, that one usually must include in the equivalent circuit one or more distributed circuit elements in addition to the usual ideal elements, such as resistors and capacitors. Important distributed circuit elements useful in equivalent circuits are described. A number of actual equivalent circuits used in the past for both liquid and solid electrolytes are presented and compared. Equivalent circuits following from detailed continuum models of the electrical response of blocking and partly conducting systems are compared, and it is shown that some of the same circuits may be used even in the presence of dc bias which usually makes the charge distribution in the system very inhomogeneous. Because frequency response data have often been inadequately analyzed, the author's general and powerful complex nonlinear least squares fitting program is now available for use by others.

(I) GENERAL INTRODUCTION

Here I shall discuss some aspects of the non-equilibrium steady-state response of systems which contain an electrical double layer (EDL), as nearly all not-purely-ohmic electrically conducting systems do. Although quasi-equilibrium measurements on EDLs with completely blocking electrodes yield primarily the total double layer differential capacitance, C_T , by itself, small-signal (s-s hereafter) ac measurements on EDL systems, which may or may not have blocking electrodes, yield much more information whether we like it or not, and we do like it when we can

* Part of the present work was presented at "The Robert A. Welch Foundation Conference on Chemical Research. XXX. Electrochemistry", which was held in Houston, TX, 3–5 November, 1986.0022-

disentangle all the information available. The basic experiment is to apply a small sinusoidal potential difference (p.d.) to the system and measure the resulting current (or vice versa). The amplitude of the applied p.d. should preferably be less than the thermal voltage $V_T \equiv kT/e$. Sometimes a larger static p.d. is applied as well, but its presence complicates the analysis of results greatly, especially in unsupported situations. Measurements are carried out over as wide a frequency range as possible, often from 10^{-4} Hz to 10^6 or 10^7 Hz, usually using automatic measuring equipment, and the impedance (p.d. divided by current) or admittance (current divided by p.d.) is calculated at each frequency. Since there is generally a phase shift between current and potential, these ratios are, by definition, complex quantities, and it is thus tautological to speak of "complex impedance" or "complex admittance" as is frequently done by many electrochemists.

Although there is nothing intrinsically new in the above approach, one that has been used in electrical engineering for seventy years or more, several new measurement and analysis elements have been added in recent years which make it far easier to carry out an experiment and to interpret its results. One such element is the development of automatic measuring equipment [1]. The combination of the basic frequency response experiment and some or all of the new elements has come to be called Impedance Spectroscopy, abbreviated IS. In this section, I shall first give a brief introduction to IS, with illustrations, then discuss some of its applications for solid and liquid systems. If one assumes, as I shall, that the experimental data are available, then it remains to present such data in a meaningful way and to analyze them so that maximum understanding of the material–electrode–interface response is gained.

(II) INTRODUCTION TO IMPEDANCE SPECTROSCOPY

Only a relatively brief background on IS will be presented because a much more detailed introduction will soon be available [1]. First, the word "impedance" in IS is a bit of a misnomer because in IS, one deals not just with impedance but with four closely related functions which can be subsumed under the umbrella designation of "immittances". Thus IS can also stand for Immittance Spectroscopy. The four functions are impedance: $Z = Z' + iZ''$, admittance: $Y = Z^{-1}$, complex dielectric constant; $\epsilon = \epsilon' - i\epsilon'' = Y/(i\omega C_c)$, and complex modulus; $M = \epsilon^{-1}$. Here ω is the angular frequency ($\omega = 2\pi f$), $i \equiv \sqrt{-1}$; and C_c is the capacitance of the measuring cell in the absence of the material of interest. Although exactly the same fitting functions and mathematical models may be used for both intrinsically conducting systems and for intrinsically non-conducting dielectric systems [2], we shall consider only conducting systems here since they are more directly relevant to the response of even completely blocking EDL situations than are pure dielectric systems.

Figure 1 shows the main elements in an IS experiment. The ideal situation, which allows estimation of the values of microscopic quantities which characterize the material–electrode system in detail, is to analyze the data by fitting them to a

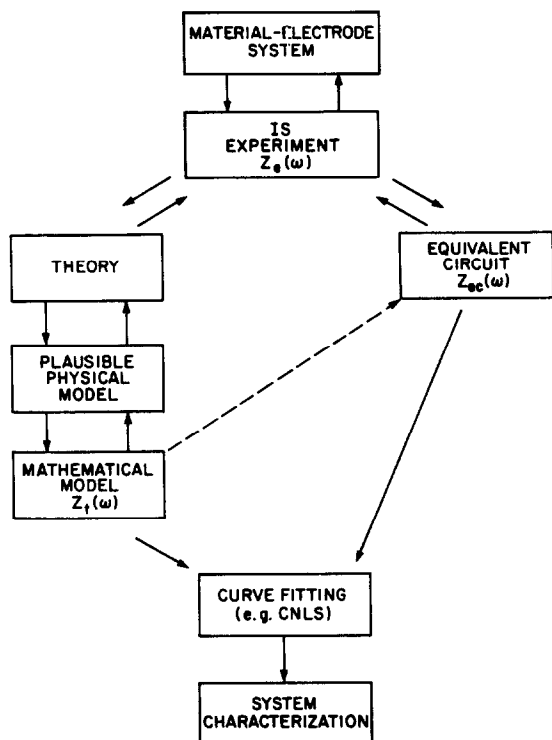


Fig. 1. Flow diagram for the measurement and characterization of a material-electrode system (reprinted by permission from John Wiley and Sons, Inc., copyright © 1987 [1]).

detailed microscopic model of the system, one which yields an explicit expression for impedance as a function of frequency and predicts the temperature dependence of all parameters present. Unfortunately, few such models are currently available, even when they are derived using continuum approximations (linear differential equations). In the absence of appropriate models one tries to make do with an equivalent electrical circuit which lumps the main physical processes occurring into macroscopic circuit elements such as capacitances, resistances and distributed circuit elements (dces). Even then there may still remain ambiguity about the most appropriate way the elements should be connected together [1,3]. Such ambiguity may often be reduced or eliminated by carrying out IS experiments on the same system at several temperatures, electrode separations, pressures, oxygen tensions, etc. This matter will be discussed further later on.

For all systems of physical interest there are two basic circuit elements which always appear. These are the high frequency limiting geometric capacitance, C_g , and the high frequency limiting resistance of the system, R_∞ , the bulk or solution resistance. They are extensive quantities and are part of the bulk response of the system as opposed to its interfacial properties. As usual, I shall ignore the distinc-

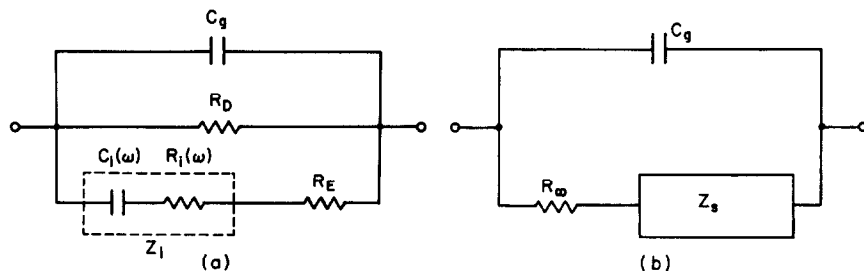


Fig. 2. Two general equivalent circuits for the small-signal ac response of a material between two conducting electrodes [4]. (a) Circuit used in early unsupported-system analysis. Here $R_{\infty}^{-1} = R_D^{-1} + R_E^{-1}$. (b) Circuit which separates out main bulk elements explicitly.

tion between such quantities and their unit area values. The product $R_{\infty}C_g \equiv \tau_D$, an intensive quantity, is just the dielectric relaxation time of the system. When neither C_g nor R_{∞} is distributed, they are frequency independent and the basic equivalent circuit involving them is that shown in Fig. 2b. The impedance Z_s represents the response of all the rest of the system and is usually the quantity of primary interest. The circuit of Fig. 2a will be discussed later.

It is worth emphasizing that C_g always spans the electrodes, as shown in the figure [5]. It is improper when $Z_s \neq 0$ just to connect C_g in parallel with R_{∞} , although this has often been done and frequently makes little actual difference to the analysis. In fact, C_g is usually entirely neglected in liquid electrolyte studies since it is generally very much smaller than the double layer capacitance, C_{DL} . The C_T which is derived from quasi-equilibrium studies is actually $C_g + C_{DL}$ when no adsorption effects occur, but it is virtually always identified as C_{DL} . In IS studies it proves important, however, to maintain the distinction between C_T and C_{DL} .

(II.a) Presentation of data

The proper presentation of data can be very helpful in indicating possible experimental errors and in suggesting the presence of various physical processes leading to the overall response. Because IS experiments often extend over a wide frequency range, it is usual to consider response as a function of the logarithm of frequency (f or ν) or angular frequency. One often sees plots of $-Z''$ and/or Z' vs. $\log(f)$, or sometimes $|Z|$ and/or ϕ vs. $\log(f)$ instead. Here, ϕ is the phase angle of the impedance; $\phi \equiv \tan^{-1}(Z''/Z')$. In the dielectric literature, plots of $\tan(\phi)$ vs. $\log(f)$ used to be common but are no longer.

One approach which is coming to be widely used is the plotting of $\text{Im}(Z) = Z''$ (or $-\text{Im}(Z) = -Z''$ in capacitive systems) vs. Z' , with frequency as a parametric variable. Such complex plane plots can be very instructive. Here, however, I wish to illustrate the usefulness of a further development in the presentation of IS data, the three-dimensional plot with perspective [6], an approach which shows the full data response in a single graph. The three dimensions of the plot are usually the real and

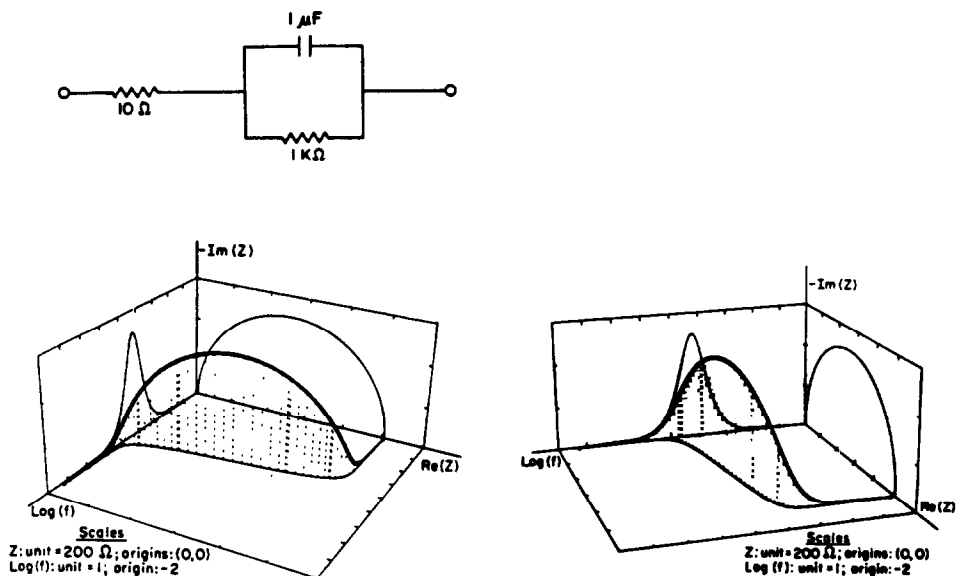


Fig. 3. Simple equivalent circuit and two 3-D perspective plots of its response viewed from different directions [6].

imaginary parts of an immittance function and $\log(f)$ or $\log(\omega)$. The alternative of using modulus and phase instead of real and imaginary parts is possible but usually turns out to be less useful. Finally, when the magnitudes of the immittance components vary by several orders of magnitude over the measured frequency range, as they often do in solid electrolyte studies, it proves useful to use logarithms of the real and imaginary parts in the 3-D plot.

Incidentally, many workers in the electrochemistry area use a non-standard definition of impedance, one which amounts to writing $Z = Z' - iZ''$ rather than $Z = Z' + iZ''$. Although this usage is convenient for systems which show capacitive rather than inductive response, it is an unwarranted redefinition of a long-established quantity. In order to avoid the hubris of Humpty-Dumpty in "Through the Looking Glass", a proper alternative is to write $Z^* = Z' - iZ''$, where Z^* is the complex conjugate impedance, and refer to the conjugate impedance in place of the ordinary impedance. When the proper definition of impedance is maintained, one may use any of the equivalent designations $-\text{Im}(Z) = -Z'' = \text{Im}(Z^*)$ in plotting.

Figure 3 shows ordinary 3-D plots for the impedance of a simple equivalent circuit, typical of those often appearing in solid or liquid electrolyte IS studies (with C_g omitted). The two plots involve different viewing positions. The heavy line represents the full response and the other three curves its projections in the three planes. In addition to showing the full response, these plots thus include all three of the different 2-D plots commonly used in the past. Note that the two parallel

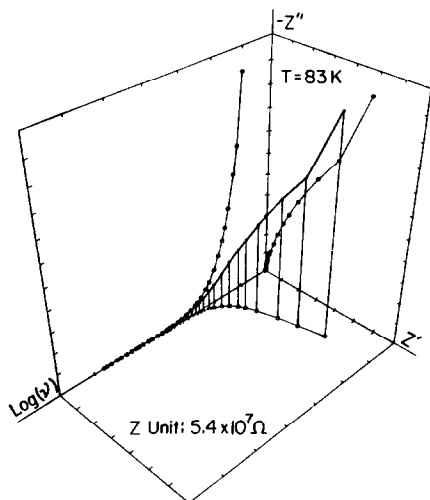


Fig. 4. Three-dimensional perspective plot of 83 K Na β -alumina impedance data [7-9].

elements in the equivalent circuit lead to a single time constant and thus to a semicircle in the complex plane, a common response shape. For even more realistic viewing, one could use a stereoscopic pair of 3-D plots.

Figures 4 and 5 illustrate the usefulness of 3-D plots in highlighting experimental errors in an IS study of the solid electrolyte Na β -alumina [7,8]. The main response curve and the complex plane projection curve in Fig. 4 show that the lowest frequency data point is inconsistent with the rest of the response. But note that the

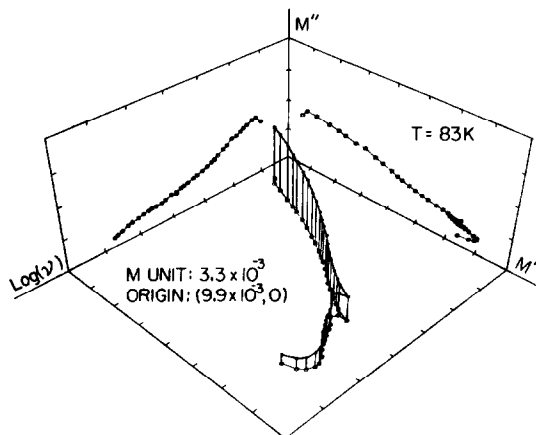


Fig. 5. Three-dimensional perspective plot of 83 K Na β -alumina complex modulus data [7-9].

projections in the other two planes, the most common sorts of plots in the past, show no trace of this error! Their use alone, as in the original data analysis [9], thus gives no clue to the presence of the error. Now the complex modulus function, $M = i\omega C_c Z$, weights the higher frequency data points more heavily than the lower frequency ones. Since many higher frequency points in Fig. 4 are not well resolved with the scale used, a modulus 3-D plot seems desirable.

Figure 5 shows that such a plot allows one to identify the same low-frequency error discussed above and to discover two new problems in higher frequency regions. Here one sees a curving back at the highest frequencies which is not theoretically likely and thus suggests the presence of measurement errors in this region. In addition, the bad glitch at somewhat lower frequencies arose because of the shift during the measurements from one type of measurement apparatus to another, evidently without adequate cross calibration in an overlap region. Here only the low frequency error shows up in the conventional projection plot of M'' vs. $\log(f)$.

These results underline the desirability of constructing 3-D plots, preferably of all four immittance functions, before any data analysis is carried out. With modern computer-controlled plotting, such plots are readily produced. Of course if bad points show up, measurements should be repeated. If that is impractical, outliers should either be eliminated or weighted weakly, and possibly mild smoothing should even be used [1].

(II.b) Complex non-linear least squares data analysis

Even the most complete data presentations are only suggestive of the processes occurring in the system investigated; a complete characterization requires that some kind of a comparison be made between the data and a theoretical model and/or reasonable equivalent circuit, as depicted in Fig. 1. In the past various graphical and/or simple mathematical fitting procedures have been carried out, often involving subtractive calculations, which can be very inaccurate. Further, these approaches generally do not analyze all the data simultaneously, and they usually yield parameter estimates without any uncertainty measures. An approach which avoids these difficulties and has great resolving power as well is that of complex nonlinear least squares (CNLS) data fitting [10]. Here all the real and imaginary data values (or the modulus and phase values) are fitted simultaneously by weighted, nonlinear least squares to a model or equivalent circuit, determining the best-fit estimates of all the free parameters, as well as first-order estimates of their standard deviations. The latter results are an essential part of the analysis since they indicate which parameters are well determined and which, if any, should be eliminated.

An illustration of the accuracy and resolution of CNLS fitting is presented in Fig. 6. Here the lumped-constant circuit shown was constructed using actual elements whose values, listed at the top, were separately measured at a few frequencies. The admittance of the full circuit was then measured with IS for many frequencies between 0.4 and 10^4 Hz. Three-D impedance and admittance plots are

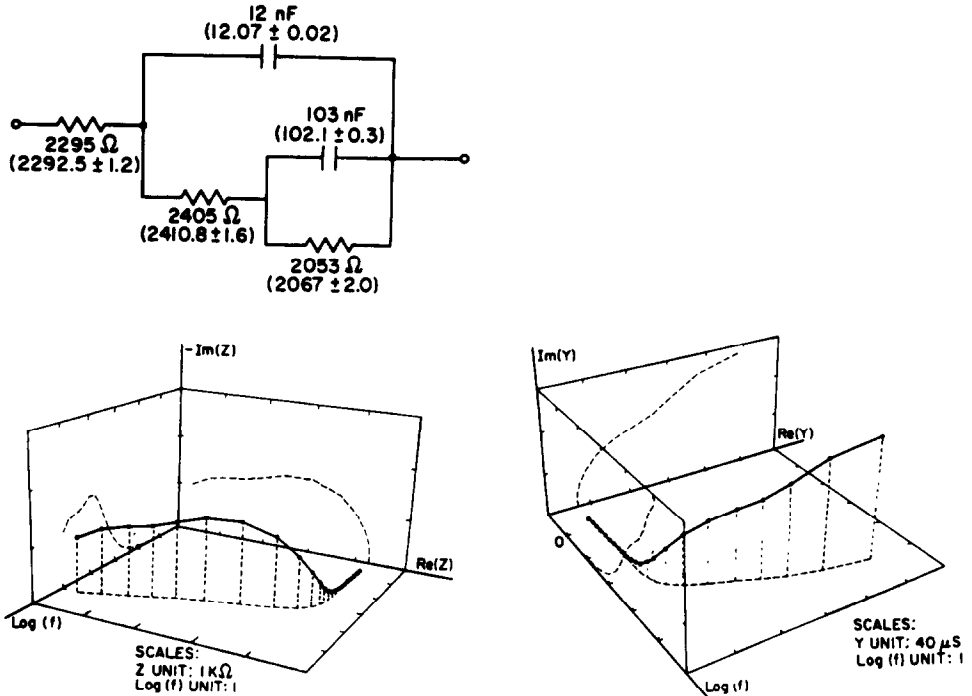


Fig. 6. Three-dimensional perspective impedance and admittance plots of the response of the lumped constant ladder network shown. CNLS fit values shown in parentheses [6].

presented in the figure and show little resolution of the two main time constants of the system. CNLS led to a very good fit of the data, however, as well as the parameter estimates and standard deviations shown in parentheses. These values agree excellently with the individually measured ones and are, in fact, probably more accurate [6,10].

Finally, Fig. 7 shows a 3-D plot and the results of a CNLS fit of data obtained from IS measurements on the solid electrolyte $\beta\text{-PbF}_2$ with platinum electrodes. Although the circuit is rather similar to that of Fig. 6, the response is of very different character, primarily because of the needed presence in the circuit of the impedance Z_D , a constant phase element (CPE), a dce. Such elements will be discussed in the next section. The small values of the relative standard deviations of the parameters obtained from the fit show that it was a good one and that all the parameters present were needed. The heavy dots in the 3-D plot are the original data points while the fit predictions are shown by solid triangles. The projection lines from these points down to the bottom plane begin to show slight discrepancies (because of imperfect fitting) at the lowest frequencies, indicating that the circuit cannot represent the data perfectly in this region. Note that seven parameters have been well estimated here. Good estimates of even more parameters can be obtained from CNLS fitting when data extend over a sufficiently wide frequency range.

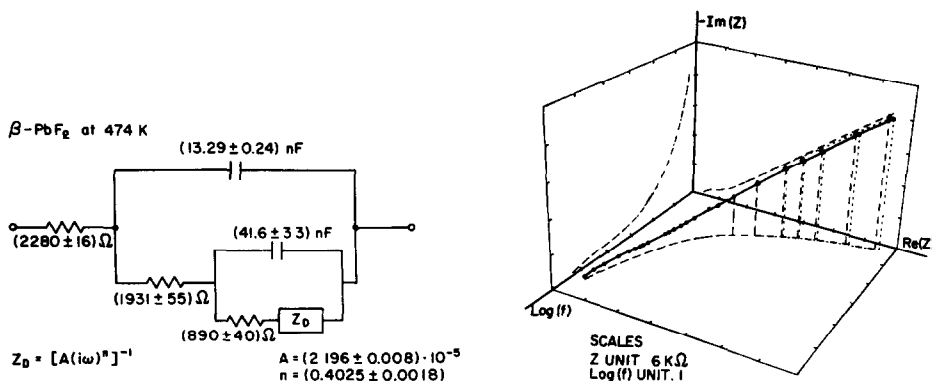


Fig. 7. Three-dimensional perspective impedance plot of β -PbF₂ data and CNLS fit response for the circuit shown [6].

There are two further sources of possible ambiguity in CNLS fitting. First, a fit may involve only a local minimum rather than the absolute least squares minimum. This problem becomes worse the larger the number of parameters to be determined in a non-linear least squares fit, but it can nearly always be circumvented by carrying out the fitting several times with very different initial values for the parameters. If the final parameter estimates are the same in all such fits, it is likely that the true least squares solution has been obtained.

Second, it is not always obvious what kind of weighting to use. In the absence of weights derived from replicating the experiment a number of times, unity weighting (UWT) or proportional weighting (PWT – the uncertainties of the components are taken proportional to their magnitudes at each point) is customarily used. Luckily, the weighting employed has only a small effect on the parameter estimates when the errors present in the fit are reasonably small [10]. It has been suggested that when the errors in the real and imaginary components are strongly correlated, modulus weighting (MWT) should be used [11]. In this case the weights for both components are just $|I|^{-2}$, where I is the immittance function being considered. Now if one fits the data in their original form without transformation to another immittance form, as one should, and if the errors are random, as one would hope, they should be uncorrelated. But transformation from a given function to its complex inverse, as from impedance to admittance, will induce some correlation in the errors of the individual components at each frequency; then for comparison of fits with these two forms, MWT may indeed be appropriate.

Computerized fitting has recently been criticized [12] because the deviations between the data and the fitting results (residuals) may show systematic behavior. Indeed they may, but this is a strength, not a weakness, of such methods as CNLS fitting! Such results provide very important information, namely that the model or equivalent circuit used in the fitting is not a perfect representation of the data. When the deviations are large enough, they are a stimulus to try to discover and

eliminate systematic errors in the data themselves and/or to try more appropriate models or equivalent circuits. Although residuals are not usually calculated and examined in the older approximate (non-computerized or non-CNLS) analysis methods, as they are as a matter of course in the CNLS approach, they are always likely to be larger than with CNLS and thus to indicate systematic behavior more frequently, sometimes when it is only an artifact of the inadequate analysis procedures used.

(III) DISTRIBUTED CIRCUIT ELEMENTS, MODELS, AND CIRCUITS

No matter how accurate and extensive one's data are, it is fair to say that the unexamined data set is not worth crowing about! Only when one has derived maximum enlightenment from it about the system involved has it served its purpose. To do so nearly always requires some comparison between the data and theoretical expectations, as discussed in the last section. A detailed model should always yield an expression for impedance vs. frequency, but it may or may not allow a useful equivalent circuit to be constructed. Whether or not such a circuit is available, the model impedance can be fit to the data using CNLS. On the other hand, when no model is available an often heuristic equivalent circuit must be used. Since real systems are distributed in space and their properties are frequently distributed as well [13], one usually needs to include one or more dces in the fitting circuit. These are elements which cannot be represented by a finite number of ordinary ideal circuit components but subsume the response of a distributed process, say diffusion, into a single expression. I shall discuss some of them briefly in the next section, and then move on to consider some models and equivalent circuits which have been used to represent and analyze the s-s ac response of supported and unsupported solid and liquid electrolyte systems. Some pertinent reviews appear in refs. 12 and 14–19.

(III.a) Some distributed circuit elements

The diffuse layer differential capacitance is itself a dce since it represents space charge response over a finite region of space. Although it shows some frequency dependence at very high frequencies (see the next section), such dependence may be neglected in the usual experimental frequency range. Many different expressions for its capacitance have been derived, depending on the exact physical conditions considered. Here I shall give only an approximate but usually adequate expression applying for the common situation of two identical, plane, parallel blocking electrodes separated by a distance l which contains many Debye lengths, L_D . Thus we shall actually be concerned, in the present case of the low-frequency-limiting differential capacitance, with two diffuse layer capacitances in series, one associated with each interface, and with C_g in parallel with the combination. As the general circuit of Fig. 2b shows, however, only in the low frequency limit can we take C_g in parallel with this combination alone. Since I shall be usually dealing with two

identical electrodes in the following, when I am, I shall define C_{dl} as the series combination of the two diffuse layer capacitances without the effect of C_g included, and take C_H as the series combination of the two inner layer capacitances. Then the (combined) double layer capacitance, C_{DL} , satisfies $C_{DL}^{-1} = C_{dl}^{-1} + C_H^{-1}$, and, for sufficiently low frequencies, $C_T = C_{DL} + C_g$. For solid electrolytes, C_H for a single interface will generally be large since it is then approximately the capacitance of two parallel plates separated by an ionic radius. It may often be set infinite to good approximation in such cases.

Although the use of two identical electrodes, a common practice for solid materials, may seem a limitation, especially for liquid electrolyte situations where half-cells are often employed, this is not the case when no static potential difference appears across the cell. Because of symmetry, two-electrode s-s ac results may be considered to be equivalent to the results which would be obtained for two identical half-cells in series, with each half-cell involving the boundary conditions of the full cell at one end and that equivalent to an ohmic electrode, undisturbed bulk concentrations, at the other. Thus full-cell solutions include both cases.

Let us ignore for the moment the effect of any C_H by taking it infinite; then C_{dl} and C_{DL} will be the same. Consider a situation where the continuum (igm) model is appropriate, and a static potential difference of ψ_a is applied across the electrodes; thus $\psi_a/2$ occurs across each diffuse layer. Then one finds for the quasi-static differential capacitance [20,21]

$$C_T = C_g [(M) \operatorname{ctnh}(M)] \cosh(\psi_a/4V_T) \quad (1)$$

Here M , the number of Debye lengths in a half cell, is defined as $l/2L_D$. This expression for C_T is intensive, as it should be for an interface-related quantity, when $M \gg 1$ and C_g plays a negligible role. When $|\psi_a/V_T| \ll 1$, one obtains the usual small-signal ac expression for C_T (not distinguished from C_{DL} by many authors) when $M \gg 1$, and one finds the extensive result $C_T = C_g$ when $M \ll 1$.

I shall now turn to the consideration of frequency response which may be associated with a distribution of relaxation times or activation energies and which applies for a single, possibly wide, dispersion region. A very important dce, whose response, or response very close to it, appears over a limited frequency range in nearly every distributed situation and in most other dces, is the constant phase element (CPE). Its admittance is of the form [1-3,13,22-25]

$$Y = A_0 (i\omega)^n \quad (2)$$

where $0 \leq n \leq 1$. This element is not physically realizable at the extremes of frequency and so should be used in conjunction with other limiting elements or in truncated form. A degenerate form of the CPE, when $n = 0.5$, is infinite-length Warburg response associated with uniform diffusion in a right half space [26]. It has been widely used in electrochemical IS studies but suffers from the same lack of physical realizability as the CPE. Its impedance is usually designated as Z_w , and it is an intensive quantity.

For a single dispersion region whose low frequency limiting resistance is R_0 and whose high frequency limiting value is R_∞ , it is convenient to introduce the normalized impedance function [2]

$$I_Z = (Z - R_\infty)/(R_0 - R_\infty) \quad (3)$$

whose limiting real values are 1 and 0. Another dce associated with uniform diffusion, but more physically plausible than the CPE or Z_W , is the finite-length Warburg, impedance Z_D , where

$$I_{ZD} = \tanh(\sqrt{is})/\sqrt{is} \quad (4)$$

and $s \equiv \omega\tau_M$ is a normalized frequency. The time constant τ_M involves mobilities or diffusion constants and the electrode separation, l . Since all real systems involve a finite separation of electrodes, Z_D , defined by eqns. (3) and (4), should always be used in place of Z_W , although formally it reduces to Z_W when $R_\infty = 0$ and $s \gg 2$. In this limit, the response is intensive, as appropriate for a region near an electrode. Note that in the zero frequency limit Z_D reduces to the impedance of a capacitor and resistor in parallel, even when $R_\infty = 0$. Here the response is extensive in character because diffusion effects then extend over the entire region between the electrodes.

The response form of eqn. (4), which is also the normalized input impedance of a finite-length shorted transmission line [27], first appeared in the present context in 1953 [28] for the unsupported situation and in 1958 [29] for the supported one. Comparisons of the two approaches [30] show that although the frequency response is of the same form, the coefficients and time constants involved are generally different, although the coefficients may be the same in one simplifying case. Franceschetti and Macdonald [27] have considered many more complicated diffusion effects in supported and unsupported small-signal response. Besides the above particular finite-length response, associated with a fast reaction at the electrode, another such limiting response appears when the diffusing entity is blocked (and possibly adsorbed) at the electrode (the analog of a finite-length transmission line with a infinite terminating resistance). Let its impedance be designated Z_{DO} . Then [27,31]

$$I_{ZDO} = \operatorname{ctnh}(\sqrt{is})/\sqrt{is} \quad (5)$$

which becomes purely capacitative in the low frequency limit but shows Z_W behavior again for $s \gg 2$. Responses of the above types can appear when the diffusing entity is either charged or neutral. Both types of response are seen fairly frequently in experimental results. It has even been suggested [31,32] that Z_{DO} response may arise in electrochromic thin films where the diffusing metallic ion is supported by electronic conduction.

Another important dce which has been widely employed in equivalent circuits for both dielectric and conductive systems leads to a complex plane curve which is a semicircle with its center depressed below the real axis, a common shape when a distribution is present [1,2,13,23,25,33]. Its I_Z representation is

$$I_Z = [1 + (is)^n]^{-1} \quad (6)$$

where s is again a normalized frequency variable. This result, which has been termed the ZARC or ZC dce, may either be considered as a response function in its own right or as the parallel combination of a resistance and a CPE. There are several other interesting combinations of a CPE and an ideal circuit element [1], but the ZC is the most common. Unfortunately, it is not physically realistic at both frequency extremes since it does not meet the criterion that its response reduce to that of a system with a single relaxation time at very low frequencies and to another single relaxation time in the limit of high frequencies [2,3,25]. In many practical cases measurements may not extend to the regions where these deficiencies become apparent, however.

Many other dces have been proposed over the years. Some of them are discussed in refs. 1, 2, 13 and 34. Here, however, it will suffice to mention three of them of current interest: the Williams–Watts (WW), Exponential Distribution of Activation Energies (EDAE), and Gaussian Distribution of Activation Energies (GDAE) dces. WW response has been found in many theoretical and experimental studies (many references are listed in the present ref. 3), although most comparisons with experiment have been inadequate, in part because the integral definitions of the WW Z' and Z'' functions are very difficult to evaluate accurately. Recently, however, an accurate approximation for WW response has been developed [35] and incorporated as an elective part of a powerful CNLS fitting program (available from the present author).

Although the GDAE and EDAE responses are also defined as integrals, they are readily evaluated numerically and are also included in the CNLS computer pro-

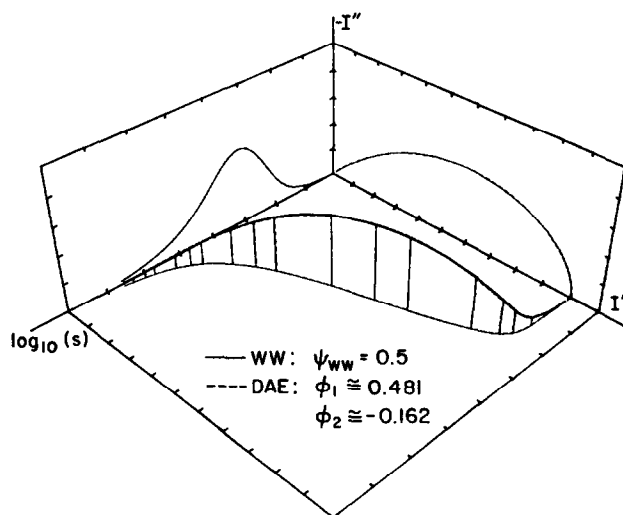


Fig. 8. Three-dimensional perspective impedance plot showing a comparison of accurate WW response (solid lines) with response obtained [3] by fitting the EDAE model to the "data" by CNLS (dashed lines).

gram. The general EDAE dce has been found to be able to fit very well the responses of nearly all the other dces which have been proposed [2,34,35]. For example, Fig. 8 shows the result of a CNLS fit of the EDAE model to accurate calculated WW response. When the system being investigated is thermally activated, as it often is, and shows evidence of distributed character (wider dispersions than arise from single-time-constant Debye response), the EDAE is probably the dce of choice, both because it is fully physically realizable and because it leads, unlike other models, to temperature dependence predictions in good agreement with experiment for the fractional frequency and time power-law exponents often found.

(III.b) Circuits and models

(III.b.1) General discussion

The presence of a supporting, or indifferent, electrolyte in supported situations decouples the charged ionic species of interest from the rest of the charges in the system, thus making its electrical effects very much easier to calculate in an approximate but usually adequately accurate way. The situation is quite different for an unsupported solid or liquid where Poisson's equation couples charges of both signs together strongly. It is thus generally much more difficult to solve electrical response problems, particularly under large signal (non-linear) conditions, in unsupported than in supported situations. Here I will primarily consider s-s solutions for unsupported conditions, finishing with some numerical results for the highly nonlinear situation where a static bias, p.d., ψ_a , is present as well as a small sinusoidal p.d.

When an equivalent circuit involves only ideal elements, it is found that some circuits with the same number of elements but with different interconnections may yield exactly the same impedance for all frequencies [3,14,18]. Three such circuits are shown in Fig. 9. The first is a series type, the second essentially parallel, and the third a hierarchical connection. The circuit elements are named differently in each circuit because they must have different values in order that the impedances of all three circuits be the same. This ambiguity may sometimes make it difficult to find the most appropriate circuit for a given situation, but it can usually be eliminated by considering the dependences of the circuit elements on one or more other experimental variables besides frequency, as mentioned in Section II. Further, it turns out that when the circuit being investigated requires the presence of one or more dces which involve CPE-like behavior the ambiguity discussed here disappears [33]. For all the circuits presented in this section, the resistances and capacitances shown are taken to be frequency independent unless otherwise noted.

In the following circuits, I shall follow prior usage in defining R_{sol} as the solution resistance for liquid materials, but I shall use R_∞ as a more general definition of the high frequency limiting bulk resistance of either a liquid or a solid material. In many electrolyte equivalent circuits the quantity C_{DL} (or C_{dl}) appears defined as just the double-layer capacitance without distinction being made between the three concepts here denoted by C_{dl} , C_{DL} , and C_T . When an expression is given for it, it is

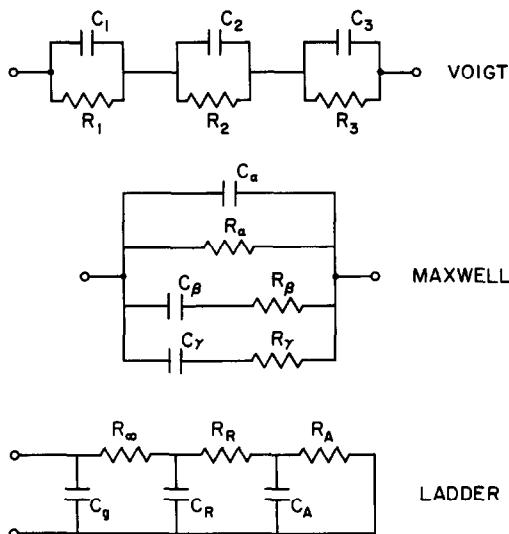


Fig. 9. Three circuits which can have exactly the same impedance–frequency relation [18]. © 1981 IEEE.

usually that of the C_T of eqn. (1) in the s - s $M \gg 1$ situation: $\epsilon_B/4\pi L_D$ for a single electrode or $\epsilon_B/8\pi L_D$ for two identical electrodes. Here ϵ_B is the dielectric constant of the bulk material. Since C_{DL} turns out to be closely associated with charge transfer reactions at an electrode involving a reaction resistance R_{ct} , or R_R , I shall often denote C_{DL} as C_R .

Figure 10a–e shows some representative equivalent circuits which have been proposed over the years as appropriate representations of the response of supported (liquid) electrolytes. The circuit of Fig. 10f is for a membrane with only charge of a single sign present in the membrane, somewhat similar to a supported situation. Other circuits are discussed in refs. 12, 14, 42, and 43. Note that only the last of the Fig. 10 circuits includes C_g and a few do not include R_{so} . Although some of these circuits have been used for data analysis, it is unfortunate that rarely have several different circuits been used to analyze the same data in order to try to discover which one is the more appropriate, and hardly any supported-situation data have been analyzed with CNLS. Such fitting and comparisons are still much needed, especially since the presence of dces in circuits of this kind eliminates most of the possibility of ambiguity discussed above. The important circuit of Fig. 10a is known as the Randles circuit (although it had already been discussed by Ershler). Randles [36] calculated expressions for R_{ct} and Z_w appropriate for the simple charge transfer reaction



where n is here the total number of electrons transferred in the reaction, and Ox and Red are oxidized and reduced species.

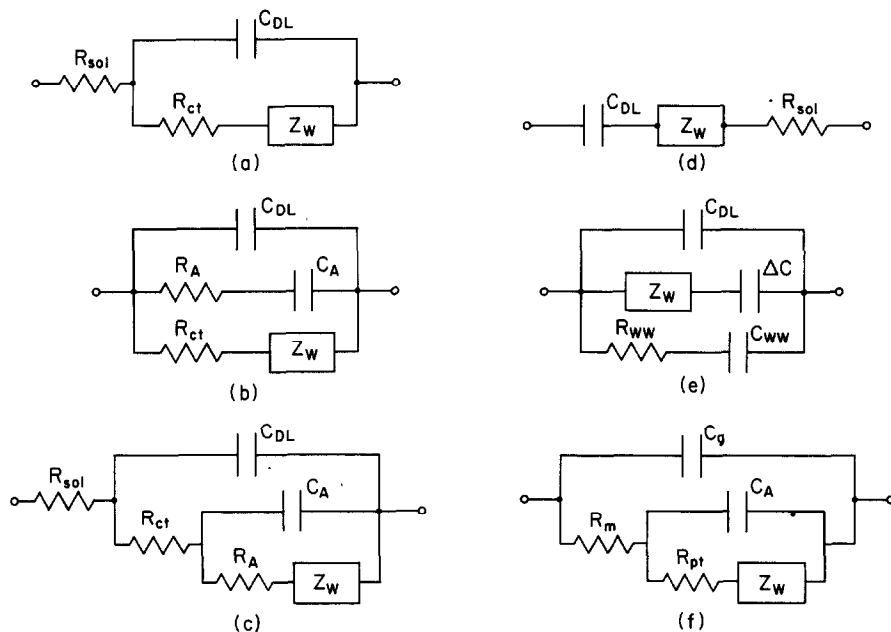


Fig. 10. Some circuits proposed for the impedance of a supported electrode-material situation; (a) "Randles" [36], (b) Laitinen and Randles [37], (c) Llopi et al. [38], (d) Barker [39], (e) Timmer et al. [40], (f) de Levie and Vukadin [41]; a membrane situation; see text. Here R_A and C_A are adsorption resistance and capacitance; ΔC is the capacitance difference between low and high frequency; R_{ww} and C_{ww} are Warburg-like elements for diffusion-controlled adsorption; R_m is a membrane (bulk) resistance; and R_{pt} is a phase transfer resistance.

An important difference between supported and unsupported conditions is associated with the mobilities of the charges. Most supported situations are present in liquid electrolytes, where both positive and negative species are mobile, usually without a tremendous difference in mobilities. Unsupported situations occur, however, in fused salts and in solids with ionic or electronic conduction. Although charges of both signs may be mobile in solids and have comparable mobilities, it is common to encounter situations where the difference in mobility is so large that the slower charges may be taken completely immobile over the time scale of the experiment.

(III.b.2) Unsupported conditions: models and theoretical results

The earliest correct treatment of the s-s frequency response of an unsupported situation appeared in 1953 [28]. It involved uni-univalent charges of arbitrary mobilities, complete blocking conditions at the two identical electrodes, and no applied static p.d. This theory and most of those discussed below apply to semiconductors as well as to solid or liquid electrolytes, but I shall emphasize the latter materials here.

No full theory of s-s frequency response for unsupported conditions with partial discharge at the electrodes appeared for some time after the above work. Such discharge occurs when a charge transfer reaction, such as that of eqn. (7), is present. Although I obtained, over a period of some years, many new theoretical results [4,15,30,44–52] incorporating the simple discharge boundary conditions of Chang and Jaffé [53], these results were made more complicated and harder to use by their analysis in terms of the equivalent circuit of Fig. 2a, and later by the use of the first circuit shown in Fig. 9. The Fig. 2a circuit isolates the zero-frequency limiting resistance of the system, R_D , and R_∞ is given by the parallel combination of R_D and R_E . By contrast, the Fig. 2b circuit separates out the high frequency elements, R_∞ and C_B , of the total response and turns out to lead to much simpler analysis and fitting [4,54].

The Chang–Jaffé (C–J) boundary conditions, which do not take an inner layer into account but do involve a pure concentration overpotential, were later generalized by Lányi [55] and the present author [15,49,50,54] by taking the discharge parameters for positive and negative charges complex and frequency dependent in such a way that the possible presence of sequential specific adsorption, as well as an electrode reaction, could be simply included. Some resulting complex plane curve shapes are shown in Fig. 11. Note that each semicircle involves a single time constant, such as $\tau_R \equiv R_R C_R$ for the reaction arc. The negative loops in Fig. 11a imply the presence of inductive or negative differential resistance and capacitance response. It has been shown [54] that the representation of the adsorption response in terms of negative resistance and capacitance is preferable to the introduction of a non-physical inductance. The rather exotic sorts of behavior shown here have actually been observed when adsorption is present.

The most complete theory using the generalized C–J boundary conditions appeared in 1978 [4]. It leads to a complicated expression for the Z_s of Fig. 2;

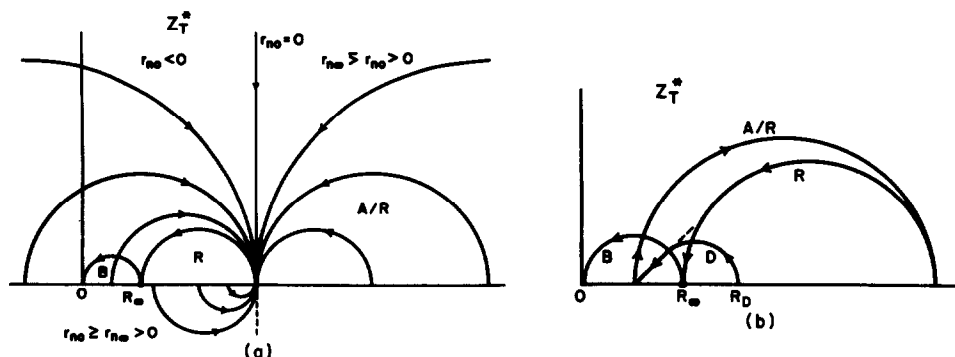


Fig. 11. Complex plane response curves for adsorption/reaction (A/R) situations [15,54]. Arrows denote direction of increasing frequency. Here R identifies a reaction arc, B a bulk arc, and D a diffusion arc. The r_n 's are rate constant parameters. The curves in (a) apply for $\pi_m \gg 1$, and those in (b) for $\pi_m = 1$ and $-\infty < r_{no} < -2$.

involves arbitrary mobilities, valence numbers, and discharge parameters; and treats both intrinsic and extrinsic conduction possibilities, with inclusion of dynamic dissociation and recombination effects. It thus includes the five important processes: charge separation near an interface, adsorption-desorption, charge transfer at an electrode, mass transport (diffusion effects), and intrinsic-extrinsic generation-recombination. Its results are too complicated to yield a useful equivalent circuit in the most general case, but such circuits may be found for some less general situations. Of course when an equivalent circuit is derived from the exact solution, expressions for the circuit elements in terms of microscopic parameters of the model follow immediately. In the present overview I shall not define in this way all the elements appearing in the equivalent circuits discussed since the detailed relations are available elsewhere.

It is possible to obtain a simple equivalent circuit for the completely blocking, intrinsic, equal valence numbers, equal mobilities case, with or without recombination. One finds [4] the exact result that $Z_s = Z_{s0}$ is made up of a capacitance $C_g t_1$ in series with a resistance $R_\infty t_1^{-1}$, where $t_1 \equiv [(M\sqrt{\psi}) \operatorname{ctnh}(M\sqrt{\psi}) - 1]$ and $\psi \equiv 1 + i\omega\tau_D$. These elements are thus frequency dependent in the $\omega \cong \tau_D^{-1}$ region where bulk effects dominate. In the usual lower frequency region where $\omega \ll \tau_D^{-1}$ and interface effects dominate, however, they are essentially frequency independent; $t_1 \cong r - 1$; and $r \equiv (M) \operatorname{ctnh}(M)$, a quantity usually much greater than unity. Then the series resistance can be neglected compared to R_∞ and the capacitance becomes just the usual $C_{dl} = C_g(r - 1)$. In the limit of low frequencies, $C_T = C_g + C_{dl} = rC_g$, in full agreement with the result of eqn. (1) when $\psi_a = 0$.

Exact results are considerably more complicated when the mobilities are unequal; then diffusion effects usually appear even in the completely blocking case [4,28,56]. The limiting low frequency finite-length-diffusion capacitance following from Z_D , sometimes called a pseudo-capacitance, is proportional to l and may be very much larger than C_{dl} [4,30,45–47]. When ψ_a is non-zero, exact analytic solution of the coupled set of non-linear differential equations which determine transient response or s-s frequency response is impossible, but Franceschetti and Macdonald [31,57,58] have solved the equations numerically for many different cases of interest. The static potential difference, ψ_a , may include an applied component and/or intrinsic Frenkel layer contributions.

The frequency response of material in finite-length half cells with one completely blocking electrode or in full cells with two such electrodes, has been calculated [31] for several values of the mobility ratio, $\pi_m \equiv \mu_n/\mu_p$, and many values of $\psi_a^* \equiv \psi_a/V_T$. Some representative complex plane impedance and admittance results for a half cell with $\pi_m = 5$ are presented in Fig. 12. The equivalent circuit of Fig. 13a was found, by CNLS fitting, to represent the data well with ψ_a zero, positive, or negative. Compare the supported-case circuit of Fig. 10d. For $\psi_a = 0$ and $\pi_m = 1$, it turns out that $Z_D = 0$, $R_1 = R_\infty$, and $C_2 = C_{dl}$, as given above. We have used the designations R_1 and C_2 here in place of R_∞ and C_{dl} to emphasize the dependences on ψ_a found for these quantities and for the parameters of Z_D . These dependences are in agreement with expectations for charge accumulation and depletion layers; that for

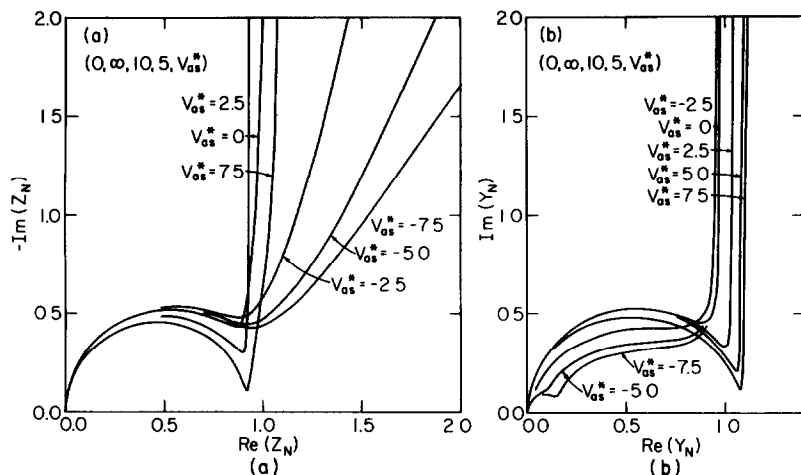


Fig. 12. Impedance (a) and admittance (b) plane plots for a half cell with a blocking electrode, $M = 10$, and $\pi_m = 5$, for several values of the normalized applied static potential difference [21].

R_1 is very small; and that for C_2 agrees very closely with appropriate quasi-static ψ_a -dependent analytic expressions [31], such as that of eqn. (1), for the cases considered.

For the $\psi_a = 0$ full-cell situation where positive charges are taken completely blocked at the electrodes and negative ones may react at the electrode with an arbitrary rate constant, k_n , Macdonald and Hull [59] have used CNLS fitting of an

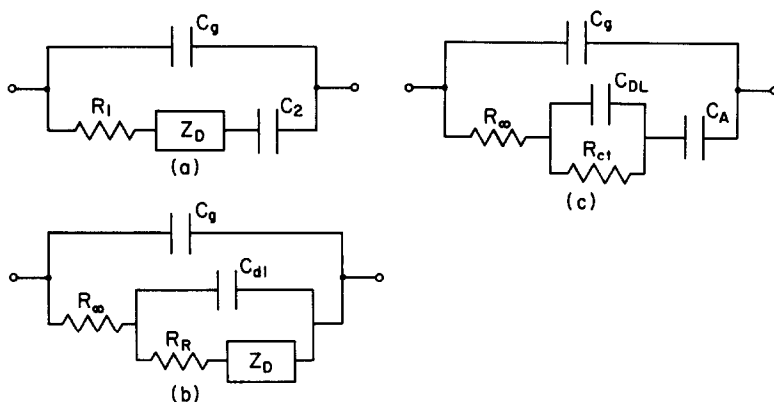


Fig. 13. (a) Equivalent circuit appropriate for one or two blocking electrodes, no specific adsorption, arbitrary π_m , and either without or with an applied static bias p.d. (b) Equivalent circuit appropriate in the small-signal, arbitrary mobilities situation [59]. (c) Equivalent circuit presented by Archer and Armstrong [17] for one-mobile blocking conditions.

appropriate circuit to the exact theoretical response [4] in order to investigate how the circuit elements depend on π_m and on recombination effects. The best fitting circuit found is shown in Fig. 13b. Notice that it would be identified as a Randles circuit (with a finite-length rather than infinite-length diffusion impedance) if supported behavior were being considered. Attention was concentrated on the $\omega\tau_D \ll 1$ frequency region, and for $\pi_m = 1$ exactly the above result for C_{dl} was found from the fitting. But C_{dl} increased rapidly for $\pi_m > 1$ and quickly dropped for $\pi_m < 1$ to about 0.7 times its $\pi_m = 1$ value, or, more precisely, to $C_g(r_1 - 1)$ for $\pi_m \ll 1$. Here $r_1 \equiv (M_1) \operatorname{ctnh}(M_1)$ and $M_1 \equiv l/L_{D1}$. The latter result may be readily understood. When $\pi_m < 0.1$, the effective Debye length is no longer that appropriate when charges of both sign are mobile, L_D , but is well approximated by the one-mobile value, $L_{D1} = \sqrt{2L_D}$.

The resistance R_R also showed interesting and important behavior. Although it is usually taken to be the reaction resistance, proportional to k_n^{-1} , it was found to be non-zero and dependent on M^{-1} even when k_n was taken infinite. Such pseudo-reaction rate response, associated with the drag of charges of one sign on those of the other sign and not with a finite reaction rate at all, can lead to entirely incorrect estimates of reaction rate values when it is unrecognized; and even when its presence is accounted for, it sets an upper limit on the maximum reaction rate value which can be reliably estimated when using CNLS to fit data as accurately as possible to the present circuit.

For the rest of the discussion I shall be concerned only with the one-mobile situation (a single species of mobile charge present) appropriate for many solids. Charge of one sign is taken immobile, and is uniformly distributed in the absence of recombination, while that of the other sign is assumed to be mobile and may react or be blocked at the electrodes. Archer and Armstrong [17] have discussed the equivalent circuit of Fig. 13c for a blocked, one-mobile situation with specific adsorption. Since it has no dc path, it allows no Faradaic current and thus no charge transfer reaction occurs. Although the exact s-s solution [4] yields a relatively simple expression for Z_s for the general one-mobile case, it still does not lead to a relatively simple equivalent circuit when recombination is possible and dissociation is incomplete. In the full dissociation limit, however, it does yield a simple circuit, that of Fig. 14 when all the Z_{Ds} are taken zero and $C_R = C_{DL} = C_{dl}$. The resulting hierarchical structure is then equivalent to the ladder network of Fig. 9 and is also equivalent in form to the supported-case circuit of Fig. 10c when one Z_D in Fig. 14 is taken non-zero and is approximated by Z_w , and C_g is ignored.

Actually, the exact solution shows that the C_g in Fig. 14 should be replaced by the impedance Z_{s0} , identified above for the completely blocking situation, but with M and r replaced by M_1 and r_1 since L_{D1} rather than L_D is the appropriate bulk Debye length in the present one-mobile case. Thus, the Fig. 14 circuit, with the restrictions above, is accurate only in the $\omega\tau_D \ll 1$ frequency region. In this region it can, however, lead to all the kinds of complex-plane curve shapes shown in Fig. 11a. Note that when $R_A = \infty$, only adsorption is present, but the structure is different from that of the Fig. 13c circuit. When R_A and Z_{D3} are both zero, one has

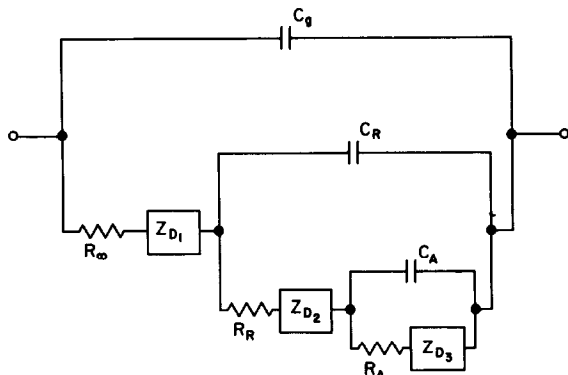


Fig. 14. General equivalent circuit. For the one-mobile situation without diffusion of reaction products, all Z_{D_s} are zero [4,18]. © 1981 IEEE.

the situation of heterogeneous reaction without adsorption. As shown above, the basic one-mobile situation involves no diffusion elements, but if a neutral reaction product diffuses in both the electrode and in the solid, at least two non-zero Z_{D_s} may need to be included in the Fig. 14 circuit [18,27,60,61], but their effects will usually show up only at very low frequencies.

One might ask how the quasi-static circuit of Fig. 9 of the preceding paper [62] for diffuse and inner layer capacitances could be extended to be consistent with the reaction/adsorption parts of Fig. 14. A tentative suggestion is as follows. When a reaction is present, C_β will be paralleled by a low resistance and their combined effects could probably be ignored in the measurable frequency range. Then if one identifies C_γ as C_H and C_{D0} as C_{dl} , their series combination is just C_R . One needs only to add R_R in series with C_A , and R_A in parallel with it, to obtain the pertinent part of the Fig. 14 circuit.

We have given little attention to the effect of C_H so far since its presence is ignored when C-J boundary conditions are employed. Luckily, a transformation of variables method has been developed [54] which allows known exact s-s solutions using even generalized C-J reaction/adsorption parameters to be transformed to solutions taking proper account of C_H and involving even more general overpotential-dependent, first-order electrode reaction kinetics than conventional Butler-Volmer (B-V) kinetics. When this method is applied for the present one-mobile case without adsorption, it leads [63,64] to the exact equivalent circuit of Fig. 15a. This circuit shows that it is possible to separate out all C_H effects into a separate series circuit which reduces to just C_H when the mobile carrier is completely blocked. Here C_{ga} is the geometric capacitance of the system excluding the two inner layer regions and $R_{\infty a}$ is the bulk resistance also excluding these regions. The exact solution for the total impedance Z_T is relatively complicated and although it could be used directly for CNLS fitting, it is useful to derive simpler approximate results [63,64].

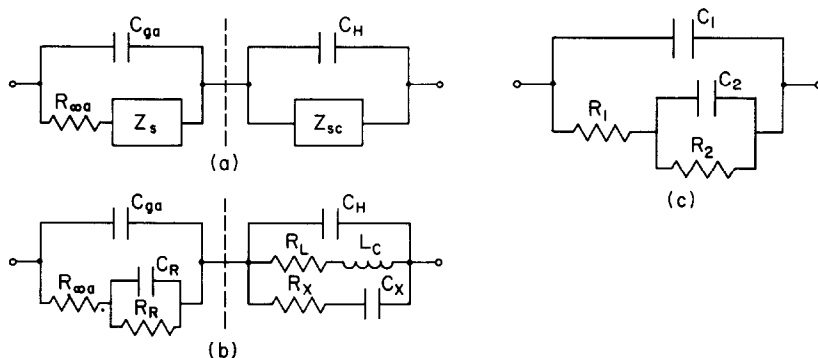


Fig. 15. Equivalent circuits which take the inner layer into account. Applicable for the one-mobile situation with general reaction kinetics [64]. (a) Exact small-signal circuit; (b) first approximate circuit; (c) second approximate circuit, appropriate with or without a Faradaic current flowing.

Such results are embodied in the equivalent circuits of Fig. 15b and 15c. That of Fig. 15b is quite accurate even up to $\omega\tau_D = 1$, while that of Fig. 15c is a good approximation up to $\omega\tau_D = 0.1$ or so. It is surprising that the complicated circuit of Fig. 15b can be well approximated by a circuit of the same form as its left half, the ordinary $C_H = 0$ solution, but this is indeed the case. The exact s-s solution shows that to a good approximation $C_1 = C_g$, and $R_1 = R_{\infty}$. Further, when the kinetics used are simplified to B-V form, it turns out [54,64] that R_2 is exactly R_R , entirely unchanged by the presence of C_H . The identity of the present unsupported-case R_R with the conventional R_{ct} reaction resistance used in supported situations and derived for B-V kinetics was pointed out long ago [47]. In addition, it has been shown [54] that the unsupported and supported expressions for the adsorption capacitance C_A are also identical.

But C_2 is not generally equal to C_{DL} , even for B-V kinetics. The results do show, however, under what specific conditions the conventional approximation is appropriate. For the general kinetics, a complicated expression for C_2 is obtained [64] which involves most of the parameters of the Fig. 15b circuit. The result is much simplified for B-V kinetics but still involves R_R . It turns out, nevertheless, that for ordinary conditions in cells with large M , it is a good approximation to set $C_2 = C_{DL}$, where $C_{DL}^{-1} = C_{dl}^{-1} + C_H^{-1}$ as usual. Then the Fig. 15c circuit is just that long used for both supported and unsupported conditions. For thin membranes with small M most of these results definitely do not apply, however, and the exact results should be used for fitting [64].

Finally, Franceschetti and I have obtained numerical solutions for the present situation with static bias applied for both full cells and half cells [58]. Typical complex plane results are shown in Fig. 16 for C-J and for B-V kinetics. Although the curves look very similar for the two cases, notice the quite different biasing currents listed. The Fig. 15c circuit was found to be quite adequate to represent the

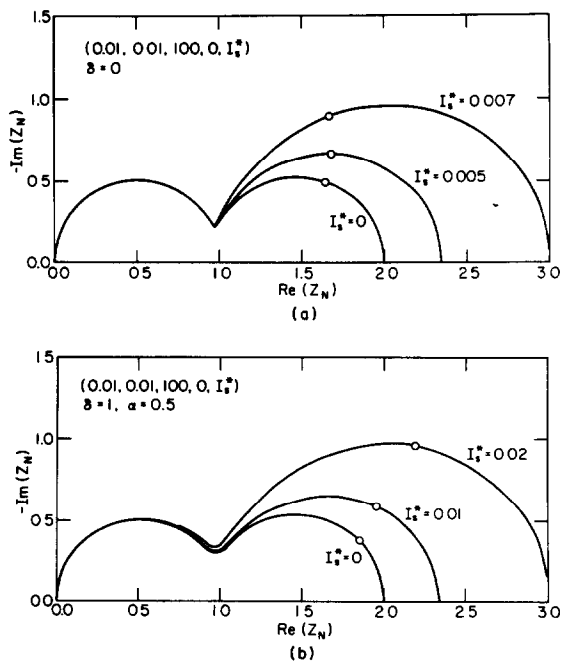


Fig. 16. Impedance plane plots for $M=100$ symmetrical cells with several biasing currents [58]. (a) Chang-Jaffé electrode kinetics; (b) Butler-Volmer electrode kinetics. These two figures were originally presented at the Spring 1979 Meeting of the Electrochemical Society, Inc. held in Boston, MA.

results, but except for C_1 the parameter values agreed only with those discussed above under zero-bias conditions. Although R_1 was found to have only small bias dependence, R_2 and C_2 varied appreciably and systematically with bias but showed considerably less variation for B-V than for C-J kinetics.

For both supported and unsupported situations, IS s-s measurements often do not agree with ideal theoretical results. For example, the R_R - C_R reaction arc appearing in the complex impedance plane is not always found to be a perfect semicircle with its center on the real axis but often is depressed, with its center below the real axis. Although the exact s-s theory yields some such depression when π_m is appreciably different from unity [47], the possible amount of depression is insufficient to explain most results. Further, "diffusion" arcs often have high-frequency power-law exponents different from the theoretical $n=0.5$ value. Although it appears that the general hierarchical circuit of Fig. 14 (with one or more Z_D s set to zero) is an appropriate starting point for fitting either supported or unsupported data, it must clearly be modified for use with data showing non-ideal behavior. One approach which often helps is to replace one or more of the ideal circuit elements or Z_D s by more general dc elements such as ZCs, WWs, or EDAEs.

Although considerable s-s frequency response data, both supported and unsupported, have been analyzed, the analysis employed has often fallen short of the state of the art. A representative list of unsupported solid materials whose data have been analyzed might include Na β -alumina (single crystal) [7,8]; (KBr)_{0.5}(KCN)_{0.5} (single crystal) [34]; polyphenylene-oxide (polymer film) [56]; β -PbF₂ (single crystal) [61]; lithium nitride (single crystal) [65]; and zirconia-yttria (polycrystalline) [66]. The data have not always been plotted in ways that show up dubious points; CNLS fitting has not always been used; and most important, too few different models or equivalent circuits have been fitted for a given set of data to allow a best choice to be established with some confidence. Much yet remains to be done, both in developing new theoretical models (e.g., see the recent work on response of three-phase electrodes [67]), and in analyzing data sets in ways worthy of them.

ACRONYM DEFINITIONS

dce	distributed circuit element
igm	ideal-gas model
p.d.	potential difference
s-s	small-signal
3-D	three dimensional
B-V	Butler-Volmer
C-J	Chang-Jaffé
CNLS	complex non-linear least squares
CPE	constant phase element
EDAE	exponential distribution of activation energies
EDL	electrical double layer
GDAE	Gaussian distribution of activation energies
IS	impedance spectroscopy
MWT	modulus weighted least squares
PWT	proportional weighted least squares
UWT	unweighted least squares
WW	Williams-Watts

ACKNOWLEDGEMENTS

First, I wish to thank the Army Research Office for their continuing support of my work. Second, it is a pleasure to acknowledge the important contributions of the many associates who have worked with me in the present area over the years, most especially D.R. Franceschetti.

REFERENCES

- 1 J.R. Macdonald (Ed.), *Impedance Spectroscopy*, Wiley-Interscience, New York, to be published.
- 2 J.R. Macdonald, *J. Appl. Phys.*, 58 (1985) 1955, 1971. In the second of these papers, the $\exp(-N_1 E)$ term in eqn. (17) should be replaced by $\exp(-\eta_1 E)$ and the \pm sign in eqn. (24) replaced by an equals sign.

- 3 J.R. Macdonald, *Revs. Mod. Phys.*, submitted.
- 4 J.R. Macdonald and D.R. Franceschetti, *J. Chem. Phys.*, 68 (1978) 1614.
- 5 J.R. Macdonald, *J. Electroanal. Chem.*, 40 (1972) 440.
- 6 J.R. Macdonald, J. Schoonman and A.P. Lehnen, *Solid State Ionics*, 5 (1981) 137.
- 7 J.R. Macdonald and G.B. Cook, *J. Electroanal. Chem.*, 168 (1984) 335.
- 8 J.R. Macdonald and G.B. Cook, *J. Electroanal. Chem.*, 193 (1985) 57.
- 9 D.P. Almond and A.R. West, *Solid State Ionics*, 3/4 (1981) 73; P.G. Bruce, A.R. West and D.P. Almond, *Solid State Ionics*, 7 (1982) 57.
- 10 J.R. Macdonald, J. Schoonman and A.P. Lehnen, *J. Electroanal. Chem.*, 131 (1982) 77.
- 11 P. Zoltowski, *J. Electroanal. Chem.*, 178 (1984) 11.
- 12 M. Sluyters-Rehbach and J.H. Sluyters in E. Yeager, J.O'M. Bockris, B.E. Conway and S. Saranagani (Eds.), *Comprehensive Treatise of Electrochemistry*, Vol. 9, Plenum Press, New York, 1984, pp. 177–292.
- 13 R.L. Hurt and J.R. Macdonald, *Solid State Ionics*, 20 (1986) 111.
- 14 R. Parsons, *Adv. Electrochem. Electrochem. Eng.*, 7 (1970) 177.
- 15 J.R. Macdonald in G.D. Mahan and W.L. Roth (Eds.), *Superionic Conductors*, Plenum Press, New York, 1976, pp. 81–97.
- 16 R.D. Armstrong, M.F. Bell and A.A. Metcalfe, *Electrochemistry*, 6 (1978) 98.
- 17 W.I. Archer and R.D. Armstrong, *Electrochemistry*, 7 (1980) 157.
- 18 J.R. Macdonald, *IEEE Trans. Electr. Insul.*, 16 (1981) 65.
- 19 R.P. Buck, *Ion-Sel. Electrode Rev.*, 4 (1982) 3.
- 20 J.R. Macdonald, *J. Chem. Phys.*, 22 (1954) 1317.
- 21 D.R. Franceschetti and J.R. Macdonald, *J. Electroanal. Chem.*, 100 (1979) 583.
- 22 H. Fricke, *Philos. Mag.*, 14 (1932) 310.
- 23 K.S. Cole and R.H. Cole, *J. Chem. Phys.*, 9 (1941) 341.
- 24 J.R. Macdonald, *Solid State Ionics*, 13 (1984) 147.
- 25 J.R. Macdonald, *Solid State Ionics*, 15 (1985) 159.
- 26 E. Warburg, *Weid. Ann. Phys. Chem.*, 67 (1899) 493.
- 27 D.R. Franceschetti and J.R. Macdonald, *J. Electroanal. Chem.*, 101 (1979) 307.
- 28 J.R. Macdonald, *Phys. Rev.*, 92 (1953) 4.
- 29 J. Llopis and F. Colom, *Proc. 8th Meeting C.I.T.C.E.*, 1956, Butterworths, London, 1958, pp. 414–427; see also P. Drossbach and J. Schulz, *Electrochim. Acta*, 9 (1964) 1391.
- 30 J.R. Macdonald, *J. Electroanal. Chem.*, 32 (1971) 317; 47 (1973) 182; 53 (174) 1.
- 31 D.R. Franceschetti and J.R. Macdonald, *J. Electrochem. Soc.*, 129 (1982) 1754.
- 32 S.H. Glarum and J.H. Marshall, *J. Electrochem. Soc.*, 127 (1980) 1467.
- 33 J.R. Macdonald and R.L. Hurt, *J. Electroanal. Chem.*, 200 (1986) 69.
- 34 J.R. Macdonald, *J. Appl. Phys.*, 61 (1987) 700.
- 35 J.R. Macdonald and R.L. Hurt, *J. Chem. Phys.*, 84 (1986) 496.
- 36 J.E.B. Randles, *Discuss. Faraday Soc.*, 1 (1947) 11.
- 37 H.A. Laitinen and J.E.B. Randles, *Trans. Faraday Soc.*, 51 (1955) 54.
- 38 J. Llopis, J. Fernández-Biarge and M. Pérez-Fernández, *Electrochim. Acta*, 1 (1959) 130.
- 39 G.C. Barker, *J. Electroanal. Chem.*, 12 (1966) 495.
- 40 B. Timmer, M. Sluyters-Rehbach and J.H. Sluyters, *J. Electroanal. Chem.*, 18 (1968) 93.
- 41 R. de Levie and D. Vukadin, *J. Electroanal. Chem.*, 62 (1975) 95.
- 42 D.C. Grahame, *J. Electrochem. Soc.*, 99 (1952) 370C.
- 43 P. Delahay, *Double Layer and Electrode Kinetics*, Interscience, New York, 1965.
- 44 J.R. Macdonald, *Trans. Faraday Soc.*, 66 (1970) 943.
- 45 J.R. Macdonald, *J. Chem. Phys.*, 54 (1971) 2026; errata 56 (1972) 681. In addition, the words “intrinsic” and “extrinsic” are improperly used in this work in place of “intensive” and “extensive”.
- 46 J.R. Macdonald, *J. Chem. Phys.*, 58 (1973) 4982; errata 60 (1974) 343.
- 47 J.R. Macdonald, *J. Chem. Phys.*, 61 (1974) 3977.
- 48 J.R. Macdonald in M. Kleitz and J. Dupuy (Eds.), *Electrode Processes in Solid State Ionics*, Reidel, Dordrecht, 1976, pp. 149–180.

- 49 J.R. Macdonald, *J. Electroanal. Chem.*, 70 (1976) 17.
- 50 J.R. Macdonald and P.W.M. Jacobs, *J. Phys. Chem. Solids*, 37 (1976) 1117.
- 51 J.R. Macdonald, D.R. Franceschetti and R. Meaudre, *J. Phys.*, C10 (1977) 1459.
- 52 J.R. Macdonald and J.A. Garber, *J. Electrochem. Soc.*, 124 (1977) 1022.
- 53 H. Chang and G. Jaffé, *J. Chem. Phys.*, 20 (1952) 354.
- 54 D.R. Franceschetti and J.R. Macdonald, *J. Electroanal. Chem.*, 82 (1977) 271.
- 55 S. Lányi, *J. Phys. Chem. Solids*, 36 (1975) 775.
- 56 S.H. Glarum and J.H. Marshall, *J. Electrochem. Soc.*, 132 (1985) 2939.
- 57 D.R. Franceschetti and J.R. Macdonald, *J. Appl. Phys.*, 50 (1979) 291.
- 58 D.R. Franceschetti and J.R. Macdonald in S. Bruckenstein, J.D.E. McIntyre, B. Miller and E. Yeager (Eds.), *Proc. Third Symp. on Electrode Processes, 1979, The Electrochemical Society, Proceedings, Vol. 80-3, 1980, pp. 94–114.*
- 59 J.R. Macdonald and C.A. Hull, *J. Electroanal. Chem.*, 165 (1984) 9.
- 60 D.R. Franceschetti, *Solid State Ionics*, 5 (1981) 613.
- 61 J. Schoonman, L.J. Still, J.R. Macdonald and D.R. Franceschetti, *Solid State Ionics*, 3/4 (1981) 365; D.R. Franceschetti, J. Schoonman and J.R. Macdonald, *ibid.*, 5 (1981) 617.
- 62 J.R. Macdonald, *J. Electroanal. Chem.*, 223 (1987) 1.
- 63 D.R. Franceschetti and J.R. Macdonald, *J. Electroanal. Chem.*, 87 (1978) 419. The term $(1 - i\Omega - \nu_n)$ in eqn. (8) of this paper should be replaced by $(1 + i\Omega - \nu_n)$.
- 64 J.R. Macdonald and D.R. Franceschetti, *J. Electroanal. Chem.*, 99 (1979) 283.
- 65 J.R. Macdonald, A. Hooper and A.P. Lehnem, *Solid State Ionics*, 6 (1982) 65.
- 66 J.E. Bauerle, *J. Phys. Chem. Solids*, 30 (1969) 2657.
- 67 D.R. Franceschetti, *Solid State Ionics*, 18/19 (1986) 101.